

XXVII International Conference “Mathematical and Computer Simulations in Mechanics of Solids and Structures”. Fundamentals of Static and Dynamic Fracture (MCM 2017)

## Effect of surgical defect localization on ultimate load-bearing capacity of human femur: finite-element energy-based assessment

S.M. Bosiakov<sup>a, \*</sup>, D.V. Alekseev<sup>a</sup>, V.V. Silberschmidt<sup>b</sup>, I.E. Shpileuski<sup>c</sup>

<sup>a</sup>Belarusian State University, 4 Nezavisimosti Avenue, Minsk 220030, Belarus

<sup>b</sup>Wolfson School of Mechanical, Electrical and Manufacturing Engineering Loughborough University, Loughborough Leicestershire, UK

---

### Abstract

Elastic properties and toughness of cortical bone tissue are non-uniformly distributed over its anatomical quadrants. This can have an effect on the bone's load-bearing capacity after a surgical resection associated with a removal of tumor-like lesions followed by formation of a sectorial bone defect. The purpose of this work is to evaluate the ultimate load-bearing capacity of the femur with the post-resection defect, taking into account various types of distributions of elastic properties and toughness in different quadrants of a cross section of the bone. The elasticity modulus of the bone tissue in the longitudinal direction of the femur is determined based on a nanoindentation test of a human femoral bone specimen. Based on numerical simulations, it is established that the most dangerous – with regard to the occurrence of a pathological fracture – is the localization of the post-resection defect, when a remaining fragment of the bone tissue is located in the anterior quadrant. In this case, the value of the ultimate load is significantly lower compared to that for other variants of localization of the post-resection defect. A non-uniform distribution of fracture toughness in the cross-section of the femur has a greater effect on the magnitude of the ultimate load than non-uniformity of elastic properties. This should be taken into account when evaluating the ultimate load, since averaging the toughness over the bone's cross-section can result in overestimations. Neglecting non-uniformity of toughness can lead to an incorrect assessment of the ultimate load and to wrong recommendations for postoperative rehabilitation of a patient.

Copyright © 2017 The Authors. Published by Elsevier B.V.  
Peer-review under responsibility of the MCM 2017 organizers.

**Keywords:** human femur; nanoindentation; modulus of elasticity; surgical resection; post-resection defect; *J*-integral; toughness; ultimate load

---

---

\* Corresponding author. Tel.: +375-17-209-5345; fax: +375-17-209-5249.  
E-mail address: [bosiakov@bsu.by](mailto:bosiakov@bsu.by)

## 1. Introduction

Bones are the main structural components of a skeleton, providing a continuous shape for a human body; they protect internal organs and transfer muscle forces. Hence, structural integrity of a bone tissue is important, since a bone can withstand loads up to a certain limit before losing its load-bearing capacity. An understanding of mechanisms of bone fracture is required for prophylaxis and prevention of injuries. The most suitable way to underpin quantitative analysis of bone's mechanical behavior is to develop adequate numerical models of a bone, as a whole, and a bone tissue, allowing studies of the causes of bone fractures, to propose ways for their prevention or healing.

Volume fractions and properties of components such as minerals, organic matrix and osteons of the bone tissue in combination with their orientation and distribution significantly influence its mechanical behavior. Differences in the orientation of the constituent components of the bone lead to its anisotropy (transverse isotropy or orthotropy) of properties, and anisotropic properties can manifest both along the length of the bone and the anatomical quadrants (or sides of the cross section of the bone) (Orías, 2005; Rho, 1996). In particular, elastic properties (Rho, 1996) and toughness (Li et al., 2013) of the cortical bone tissue are non-uniform along the bone's circumference (in different anatomical quadrants).

Different properties of bone tissue for different quadrants of the bone cross-section can influence the bone's load-carrying capacity after surgical resection (removal of a tumor-like lesion with formation of a sectorial bone defect). This is due to the fact that a part of the bone remaining after the operation is loaded partially or fully, corresponding its position in the cross section of the bone. Figure 1 shows the scheme of surgical resection.

As a result of surgical resection, the strength of the segment decrease and there is a risk of a pathological bone fracture at the resection level. The aim of this study is to evaluate the ultimate load on the femur with post-resection defect, taking into account the various elastic properties and toughness of bone tissue in different quadrants of the cross section of the bone. The elasticity modulus of bone tissue is determined using the nanoindentation test of the human femoral bone sample.

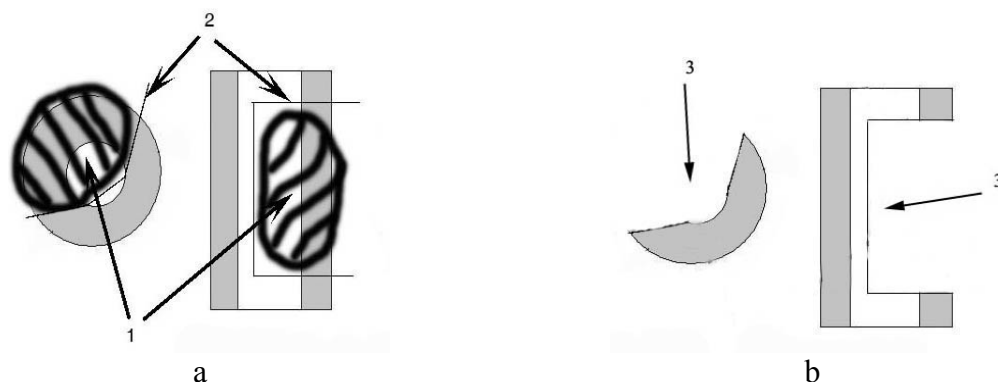


Fig. 1. Scheme of a surgical resection: (a) fragment of tubular bone before resection; (b) fragment of tubular bone after resection (1 - tumor, 2 – bone-cutting lines; 3 - post-resection defect)

## 2. Materials and methods

### 2.1. Nanoindentation of sample of bone tissue

#### *Sample preparation.*

The sample for experiment was cut from the middle third of a human dry femur (male, 49 years, the sample was provided by the Republican Scientific and Practical Centre for Traumatology and Orthopedics, Minsk, Belarus). Grinding and polishing of bone specimens was performed according to the ANSI standard (grinding with paper

granularity 240, 400, 600 and 1200, finishing with a fabric with polishing slurry with a particle size of 3  $\mu\text{m}$  and 1  $\mu\text{m}$ ).

### *Nanoindentation process*

For experiments in this study, a NanoTest 600 testing machine (Loughborough University, UK) was used. Nanoindentation was carried out at a temperature of 23.3°C and relative humidity of air of 31.7%. For indentation, a spherical diamond tip with a radius of 25  $\mu\text{m}$  and an indenting head for a small load of 0.1–500 mN was employed. The sample was glued horizontally to a holder and attached to a front end of the system opposite to the indenter tip. Using the built-in microscope, the indenter was placed in the desired position. Tests were performed in the load-control mode. The maximum load for each side was 222.3 mN, the maximum depth was approx. 2220 nm with a loading speed of 2 mN/s, and a time delay of 60 seconds. Five to seven cycles of loading-unloading were carried out. The indents into the sample were performed in central regions of its anterior (A), posterior (P), medial (M) and lateral (L) quadrants.

### *2.2. Finite-element modelling*

Computed tomography of the femur and bones of the lower leg was performed on a spiral X-ray tomograph Siemens Somatom Emotion 16, with the cutoff step of 2 mm. Finite-element modelling was performed using ScanIP (Simpleware Ltd., UK), CATIA V5 (Dassault Systèmes, France) and ANSYS Workbench 14.0 (ANSYS Inc., USA).

The load on the femur was applied along the biomechanical axis passing from the upper pole of the femoral head to the middle of the distance between the extreme lower sections of the condyles of the femur (Letter to the editor, 2002; Yoshioka et al., 1987). The region of application of the load was the third part of the upper segment of the head of the femur. The boundary conditions were defined in such a way that the femoral head (the acetabular contact area) and the lower sections of the condyles of the femur (the sites of contact with the condyles of the tibia) were rigidly embedded (Letter to the editor, 2002).

In numerical simulations, a bone defect was located in the middle third of the femur in various quadrants of the cross section. The angular dimensions of the defects, irrespective of the quadrant, were 270°, while its linear dimensions were 50.2 mm. Variants of the location of the bone defect in the cross section of the femur are schematically presented in Figure 2. The femoral bone after surgical resection, corresponding to the variant 2 of the bone defect location (see Figure 2), is shown in Figure 3.

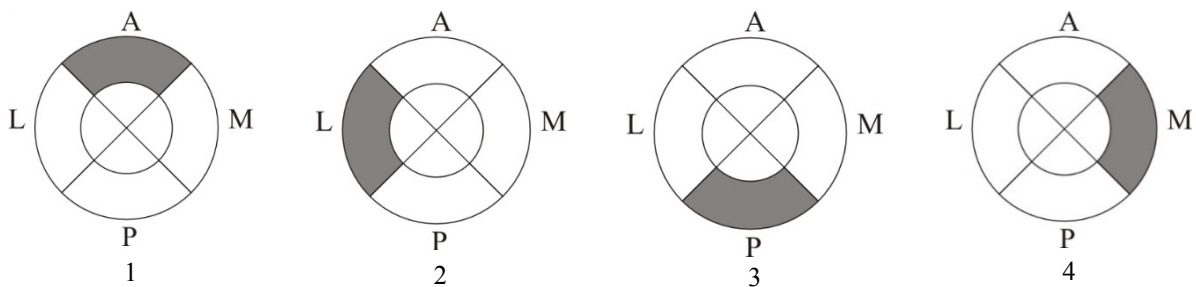


Fig. 2. Schematics of location of bone defect in different quadrants of cross section of femur: (1) anterior; (2) lateral; (3) posterior; (4) medial (the quadrant with the fragment of bone tissue left after surgical resection is highlighted in gray)

The bone tissue was modelled as a homogeneous linear isotropic medium with the Poisson's ratio equal to 0.3 (Tanne and Sakuda, 1991). The bone's elasticity modulus was set to be the same for the entire bone as a whole in accordance with the results of the nanoindentation test, depending on the location of the bone defect.

The finite-element meshing of the femoral bone model was carried out automatically, except for the regions in the direct vicinity of the bone defect, using hexagonal and tetrahedral elements. The maximum size of the element for the femur was 5.0 mm (excluding the areas in the area of the bone defect). The finite-element meshing of the regions around the defect – stress concentrators – was performed using spheres of influence in ANSYS Tools; the maximum size of the element in these areas was 0.2 mm. An analysis of the net convergence for the model of the femur was carried out in (Bosiakov et al., 2016).

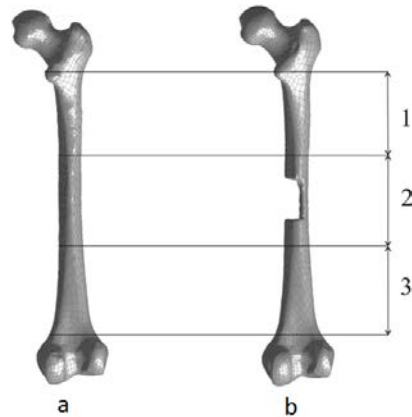


Fig. 3. Models of intact femur (a) and femur with post-resection defect (b) after surgical resection and with remaining fragment of bone tissue in lateral quadrant (1 - upper third, 2 - middle third, 3 - lower third)

### 3. Results

#### 3.1. Mechanical properties: Elasticity moduli

Based on the results of indentation tests, elasticity moduli in the longitudinal direction (along the anatomical axis of the femur (Letter to the editor, 2002)) were determined. The experimental data were processed using the elastic-plastic theory by Oliver and Pharr (1992). Figures 4 and 5 demonstrate the average values of the elasticity moduli and the standard deviations, as well as the distribution of elasticity moduli for different quadrants of the femoral specimen.

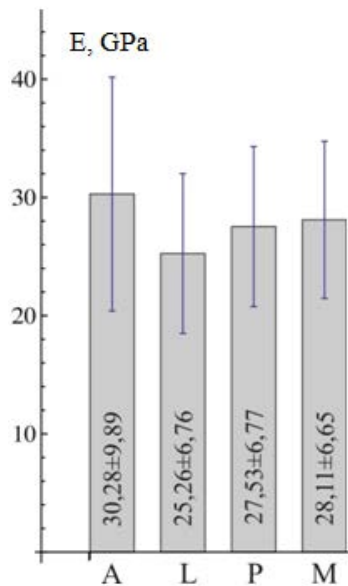


Fig. 4. Average values of elasticity modulus of femoral specimen: A - anterior quadrant, P - posterior quadrant, M - medial quadrant, L - lateral quadrant (the lengths of the segments in the diagrams correspond to the value of the standard deviation)

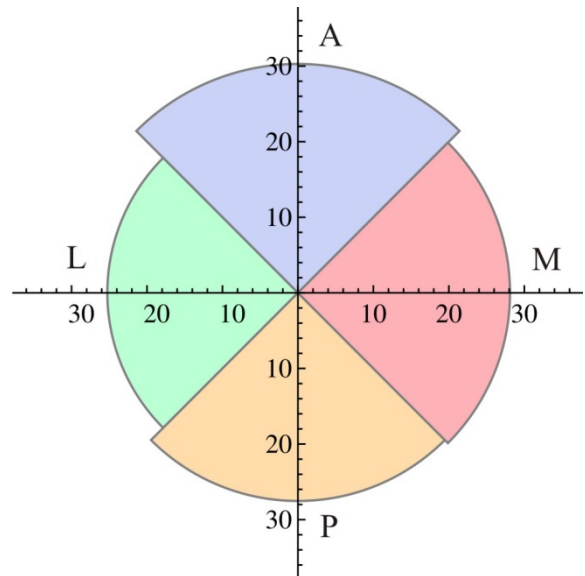


Fig. 5. Distribution of elasticity moduli for different quadrants of femur: A - anterior quadrant, P - posterior quadrant, M - medial quadrant, L - lateral quadrant (the radius of the sector correspond to the average value of the elasticity modulus for the corresponding quadrant of the sample, shown in Figure 2)

Apparently, the largest value of the elasticity modulus was observed in the anterior quadrant, the smallest value – in the lateral quadrant of the sample.

### 3.2. Evaluation of ultimate load.

The ultimate load was assessed on the basis of calculation of  $J$ -integrals in the sectorial-defect areas for four variants of the location of the bone defect (see Figure 2). The load was assumed to be limiting if the  $J$ -integral reached the critical value  $J_C$ , experimentally determined for cortical bone tissue in (Simin et al., 2013). The range of values of the limiting load on the femur with the post-resection defect was determined for variants 1-4 of the location of the bone defect in three cases. In the first case, the elasticity modulus of the bone tissue of the entire femur took one of the values determined in the nanoindentation test (see Figures 4 and 5), while the  $J_C$  values were different for all anatomical quadrants in accordance with (Simin et al., 2013). In the second case, the elasticity modulus for the whole bone was also assumed to be of the values of the elasticity moduli, but an average the value  $\langle J_C \rangle$ , calculated on the basis of the results of Simin et al. (2013) was assumed for all the quadrants. In the third case, both the elasticity modulus of the bone tissue and  $J_C$  took the averaged values. The results of determining the maximum load for the above three cases are presented in Tables 1-3.

Table 1. Ultimate load values for femur and standard deviation for various variants of localization of post-resection defect

Defect localization	1	2	3	4
Elasticity modulus of femur in general, GPa	30.28±9.89	25.26±6.76	27.53±6.77	28.11±6.65
$J_C$ , N/m [3]	4509.1±422.1	5661.6±452.7	3876.7±847.3	5925.5±802.9
Ultimate load, N	510±30	1180±35	1030±45	1120±55

Table 2. Ultimate load values for femur and standard deviation for various variants of localization of post-resection defect for uniform distribution of  $\langle J_C \rangle = 4993.23 \pm 631.25$  N/m (Simin et al., 2013)

Defect localization	1	2	3	4
Elasticity modulus of femur in general, GPa	30.28±9.89	25.26±6.76	27.53±6.77	28.11±6.65
Ultimate load, N	500±35	790±45	1130±30	1020±45

Table 3. Ultimate load values for femur and standard deviation for various variants of localization of post-resection defect for uniform distribution of both  $\langle J_C \rangle = 4993.23 \pm 631.25$  N/m (Simin et al., 2013) and elasticity modulus of femur (27.30±7.52 GPa)

Defect localization	1	2	3	4
Ultimate load, N	525±25	825±25	1205±75	1000±50

The results presented in Tables 1-3 for the four analyzed variants of bone-defect localization and the three cases for assessment of the ultimate load are systematized in the diagram shown in Figure 6.

As it follows from Tables 1-3 and 6 that an anisotropic distribution of impact strength and mechanical properties of bone tissue for various anatomical quadrants can have a significant effect on the value of the ultimate load on the femur with post-resection defect. Particularly significant is the effect of anisotropy of impact strength on the magnitude of the maximum load for variant 2 of localization of post-resection defect (with localization of the bone tissue fragment remaining in the lateral quadrant after resection). Averaging the toughness in the cross section of the femur leads to a significant reduction in the ultimate load for this variant. Also, the value of the ultimate load is averaged when averaging the impact strength in case of variant 4 of post-resection defect localization (the fragment of bone tissue remaining after surgical resection is located in the medial quadrant). But a decrease in the value of the limiting load is inessential in this case. The most dangerous consequences can be averaging the toughness when assessing the ultimate load for option 3 of the location of the post-resection defect (the remaining fragment of the bone tissue is located in the posterior quadrant). In this case, the magnitude of the ultimate load is too high after averaging over the load value estimated with allowance for different values of the toughness for different anatomical quadrants. Thus, neglecting the anisotropy of toughness can lead to an incorrect assessment of the ultimate load value, which can lead to incorrect recommendations for postoperative rehabilitation of the patient. In particular, a discharge regime for

the patient can be assigned, if necessary, to reinforce the femur. For variant 1 localization of post-resection defect (the remaining fragment of bone tissue is located in the anterior quadrant), the anisotropic distribution of impact strength and mechanical properties in the femoral cross section has practically no effect on the magnitude of the ultimate load. Also note that it can be seen from Fig. 6 that the anisotropic distribution of elastic properties in the cross-section of the femur has a lesser effect on the magnitude of the ultimate load than the anisotropy of the toughness.

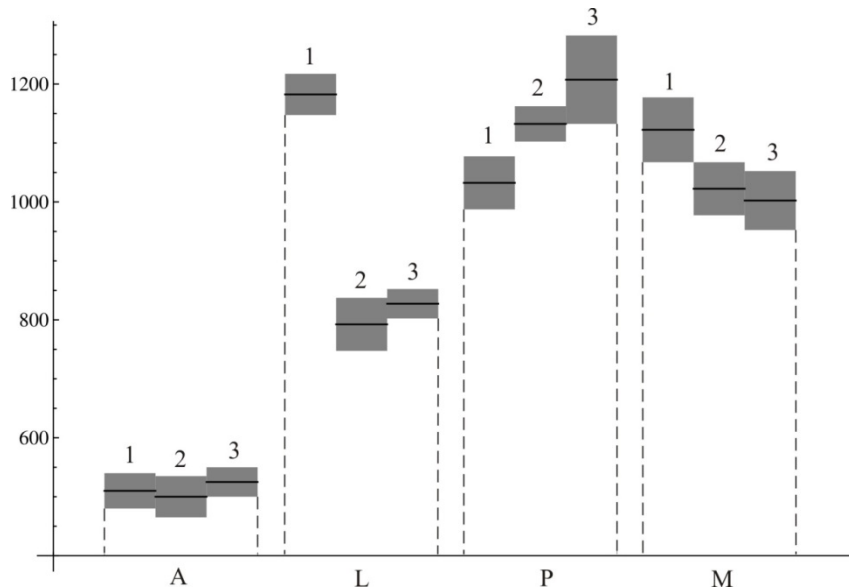


Fig. 6. Ultimate load value for femur with post-resection defect for different variants of localization of bone defect and three types of evaluation: (1) taking into account different mechanical properties and values of  $J_C$  for different anatomical quadrants; (2) taking into account different mechanical properties and assuming single averaged value of  $\langle J_C \rangle$  for different anatomical quadrants; (3) assuming averaged values for both elasticity modulus and  $J_C$  for different anatomical quadrants) (A, L, P and M correspond to variants 1, 2, 3 and 4 of the post-resection defect location in Figure 2. The solid line corresponds to the average load value; the standard deviation is indicated in gray).

#### 4. Conclusions

The following conclusions can be drawn from the undertaken research:

- Variant 1 of the post-resection defect localization (the remaining fragment of the bone tissue located in the anterior quadrant) is the most dangerous with regard to the probability of a pathological fracture, with the value of the ultimate load being significantly lower in this case in comparison with the remaining variants of the defect's localization.
- In cases of bone-defect localization when the fragment of the bone tissue remaining after the surgical resection is located in lateral, posterior or medial quadrants, the values of the limiting load are of similar magnitude.
- The non-uniform distribution of elastic properties in the cross-section of the femur has a smaller effect on the value of ultimate load than non-uniformity of strength.
- The non-uniform distribution of bone-tissue toughness for different anatomical quadrants can have a significant effect on the value of the ultimate load of the femur with the post-resection defect. The effect of the toughness non-uniformity on the magnitude of the ultimate load is particularly important for the case of localization of the bone fragment remaining after resection in the lateral, medial or posterior quadrants.
- The non-uniform distribution of toughness should be considered when assessing the ultimate load value for the case with the remaining bone-tissue fragment located in the posterior quadrant. In this case, using the averaged value of toughness can lead to a significant overestimation for the ultimate load.
- Neglecting non-uniformity of fracture toughness can lead to incorrect assessment of the ultimate load value and wrong recommendations for postoperative rehabilitation of the patient.

## Acknowledgements

Financial support of the FP7 IRSES project TAMER “Trans-Atlantic Micromechanics Evolving Research “Materials containing inhomogeneities of diverse physical properties, shapes and orientations” (Grant no. IRSES-GA-2013-610547) is gratefully acknowledged.

## References

- Bosiakov S., Alekseev D., Koroleva A., Rogosin S., Shpileuski I., Silberschmidt V., Demirci E., Dorozhko A., 2016. Assessment of ultimate load for human femur after surgical resection: comparative experiment. In: *Analytic methods of analysis and differential equations: AMADE 2015* S.V. Rogosin, M.V. Dubatovskaya (Eds.). Cambridge Scientific Publishers, pp. 27-36.
- Letter to the editor, 2002. ISB recommendation on definitions of joint coordinate system of various joints for the reporting of human joint motion—part I: ankle, hip, and spine. *Journal of Biomechanics* 35, 543–548.
- Li S., Demirci E., Silberschmidt V.V. , 2013. Variability and anisotropy of mechanical behaviour of cortical bone in tension and compression // *Journal of Mechanical Behavior of Biomedical Materials* 21, 109-120.
- Oliver W.C., Pharr G.M., 1992. An improved technique for determining hardness and elastic modulus using load and displacement sensing indentation experiments. *Journal of Materials Research* 7, pp. 1564-1583.
- Orias A.A.E. The relationship between the mechanical anisotropy of human cortical bone tissue and its microstructure / Dissertation. Notre Dame, Indiana, USA. 2005. 142 pp.
- Rho J.-Y., 1996. An ultrasonic method for measuring the elastic properties of human tibial cortical and cancellous bone. *Ultrasonics* 34, 777-783.
- Tanne T., Sakuda M., 1991. Biomechanical and clinical changes of the craniofacial complex from orthopedic maxillary protraction. *Angle Orthod.*, 61, 145–152.
- Yoshioka Y., Siu D., Cooke D.V., Chir B., 1987. The anatomy and functional axes of the femur. *J. Bone Join. Surg.* 69-A, 873-880.